JOURNAL OF GEOPHYSICAL RESEARCH, VOL. 113, A11206, doi:10.1029/2008JA013352, 2008

Enceladus: A potential source of ammonia products and molecular nitrogen for Saturn's magnetosphere

H. T. Smith,[1,2] M. Shappirio,[3] R. E. Johnson,[1] D. Reisenfeld,[4] E. C. Sittler,[3] F. J. Crary,[5] D. J. McComas,[5] and D. T. Young[5]

Received 2 May 2008; revised 21 July 2008; accepted 25 August 2008; published 12 November 2008.

[1] The detection of nitrogen species in Saturn's magnetosphere could, in principle, provide clues to the origin and evolution of its satellites and tenuous rings. Smith et al. (2005) first identified low-energy N^+ using the Cassini Plasma Spectrometer (CAPS). N^+ was predominantly seen in the Saturn's inner magnetosphere (<~14 Rs), indicating an Enceladus nitrogen source rather than the expected Titan source. However, the parent molecular species was not confirmed. Subsequent modeling showed that a small N_2 source at Enceladus consistent with ion neutral mass spectrometer observations could produce the observed spatial distribution of N^+. Considering the significance of understanding the Enceladus plumes, identifying the molecular parent for the observed N^+ (N_2 or NH_x) can provide clues to the subsurface composition of Enceladus and the processes generating this plume activity. In this paper, we expand on the work of Smith et al. (2007) to identify the source molecules for nitrogen ions detected in Saturn's inner magnetosphere. We conduct an extensive study of all available CAPS data to determine if N_2^+ or ammonia is the parent molecule for these nitrogen ions. We present evidence for the detection of product ions (NH_x^+), likely from ammonia, and provide upper limits on the amount of N_2^+ that may be present in the plasma in the inner magnetosphere.

Citation: Smith, H. T., M. Shappirio, R. E. Johnson, D. Reisenfeld, E. C. Sittler, F. J. Crary, D. J. McComas, and D. T. Young (2008), Enceladus: A potential source of ammonia products and molecular nitrogen for Saturn's magnetosphere, *J. Geophys. Res.*, *113*, A11206, doi:10.1029/2008JA013352.

1. Introduction

[2] The presence of nitrogen species in Saturn's magnetosphere can, in principle, provide important insight into the origin and evolution of its satellites and tenuous rings. Prior to the Cassini spacecraft arrival at Saturn, knowledge of the Saturnian system was limited to three fly-bys (Pioneer 11, Voyagers 1 & 2), Hubble Space Telescope and Earth-based observations. On the basis of this information, early expectations were that the vast majority of nitrogen ions in the Saturn system would be produced from the dense, relatively unprotected, nitrogen-rich atmosphere of Saturn's largest moon, Titan [*Barbosa*, 1987; *Ip*, 1997; *Smith et al.*, 2004].

[3] With the arrival of the Cassini spacecraft at Saturn in July 2004 a comprehensive study of nitrogen sources and sinks became possible. However, neutral nitrogen densities in Saturn's magnetosphere were too low for direct in-situ detection by Cassini (or ground based) instruments, except very close to the parent bodies. For this reason, the Cassini Plasma Spectrometer (CAPS) has been used to detect nitrogen-containing ions from the hypothesized neutral nitrogen torus [*Smith et al.*, 2004]. The CAPS contains an Ion Mass Spectrometer (IMS) capable of detecting ions with energies between 1 eV and 50 keV with mass per charge ratios (M/Q) between 1 and 100 amu/e. The energy resolution (dE/E) is ~0.17 while the mass resolution (M/dM) is ~60 [*Young et al.*, 2004]. The IMS collects ions in a selected energy/charge range and determines the time of flight (TOF) from which the ion mass/charge can be determined.

[4] *Smith et al.* [2005] first identified low-energy N^+ using the IMS. However, N^+ was not detected close to Titan's orbital radius, as expected, but rather much closer to Saturn in the inner magnetosphere (<~14 Rs). In these initial results, these authors reported that nitrogen ions are most abundant near the orbit of Enceladus which they proposed was the principal source. Abundances were generally around 10% of the heavy ion population although the relative amount of N^+ could be somewhat higher near Enceladus' orbit. Because of nitrogen's volatility, this finding became even more interesting with the subsequent detection of activity at Enceladus in the form of plumes emanating from a locally warm region near the south pole [*Porco et al.*, 2006], a region also containing geologic features referred to as the "tiger stripes".

[1]Engineering Physics, University of Virginia, Charlottesville, Virginia, USA.
[2]Applied Physics Laboratory, Johns Hopkins University, Laurel, Maryland, USA.
[3]NASA Goddard Space Flight Center, Greenbelt, Maryland, USA.
[4]Department of Physics and Astronomy, University of Montana, Missoula, Montana, USA.
[5]Division of Space Science and Engineering, Southwest Research Institute, San Antonio, Texas, USA.

0148-0227/08/2008JA013352$09.00

[5] Modeling the N^+ density variation with distance from Saturn and the N^+ to water ion density ratio using data from a number of Cassini orbits, *Smith et al.* [2007] confirmed their earlier suggestion that Enceladus was the likely source of the observed nitrogen ions. These authors also attempted to model the parent molecule of these ions. During a close fly-by of Enceladus, the Cassini ion neutral mass spectrometer (INMS) detected neutral particles with an atomic mass of 28 in the plumes [*Waite et al.*, 2005] at about a 4% relative amount. However, whether this was N_2 or CO could not be determined, although constraints based on Cassini Visual and Infrared Mapping Spectrometer (VIMS) and Ultraviolet Imaging Spectrograph (UVIS) observations suggested that N_2 was the most likely candidate [*Waite et al.*, 2006]. Smith et al. positively detected N^+ but not N_2^+, while the INMS observations reported atomic mass 28 but not 14. Because the N_2 dissociation lifetime is shorter than its ionization lifetime, modeling showed that a small N_2 source at Enceladus could produce the observed spatial distribution of N^+ without an obvious N_2^+ detection because it is extremely difficult to detect such small amounts of N_2^+ using CAPS IMS.

[6] The physical processes producing Enceladus plume activity are not well understood. Possible mechanisms range from tidal heating [*Nimmo and Pappalardo*, 2006] to the presence of subsurface ammonia (NH_3) which would lower the melting point of a hypothetical reservoir of water ice [*Stevenson*, 1982; *Squyres et al.*, 1983; *Matson et al.*, 2007]. Therefore establishing the presence or absence of NH_3 is critical for understanding the nature of the plume source. No confirmed ammonia detection at Enceladus has yet been reported. Lack of detection might not be surprising, however, because NH_3 should be present in only small amounts [*Verbiscer et al.*, 2006] and direct observation by reflectance in the surface ice is hindered because it is a volatile species that can be depleted thermally or by sputtering [*Lanzerotti et al.*, 1984]. Given the volatility of ammonia and the relatively large neutral densities required for direct Cassini INMS observation of NH_3 ($>10^4/cm^3$, *Waite et al.*, 2004), CAPS IMS observations are critical because they are capable of detecting small amounts [as low as $10^{-3}/cm^3$, *Young et al.*, 2005] of ammonia product ions (NH_x^+ where x = 1–4).

[7] Identifying the molecular parent for the observed N^+ (N_2 or NH_x) can therefore provide clues to the subsurface composition of Enceladus and the processes generating this plume activity. In this study, we present the results of a comprehensive examination of CAPS IMS data that indicates the presence of NH_x^+ as well as support for the presence of N_2^+, two species that are indicative of the parent molecules for the N^+ observed in Saturn's inner magnetosphere.

2. Ammonia Products

[8] Given the potential significance presented by the absence or presence of ammonia in Saturn's inner magnetosphere detection of NH_x^+ is very important. The INMS placed upper limits on neutral ammonia detection in the Enceladus plume of 0.5% [*Waite et al.*, 2006]. Considering these relatively small concentrations, detection of neutral ammonia molecules away from the plume itself is expected to be very difficult. However, products formed from the ionization/charge exchange of neutral ammonia might be detectable at relatively low densities by the CAPS.

[9] The CAPS IMS measures ion TOF using two methods each with its own detector: the Straight-Through (ST) and the Linear Electric field (LEF). The ST is relatively more sensitive but has lower mass resolution (M/dM ~8). Lower mass resolution is appropriate for many species, but not sufficient for this study because ammonia products are located in the same area of the TOF spectrum as the much more abundant water-group ions that dominate Saturn's magnetosphere. This characteristic makes it very difficult to separate ammonia ions with any significant confidence level.

[10] The LEF detector has much better mass resolution, however with a lower efficiency than the ST detector. In the LEF detector, the N^+ spectral peak is well resolved from products in the water group peak. Additionally, the signal from nitrogen ions derived from ammonia products form a shoulder on the atomic N^+ peak that can theoretically be resolved. Therefore, although detection is challenging, mass resolution is sufficient to identify the presence of ammonia products. Unfortunately, even with this better mass resolution, the signals are so low that it is difficult to conclusively identify ammonia when the relative abundance of ammonia to N^+ is less than ~50%.

[11] We have developed a method to analyze spectra accumulated over long periods of time in such a way that we can confidently identify the presence or absence of relatively small amounts of ammonia products. In particular, the LEF detector is constructed such that atomic species have narrow TOF peaks while molecular species have noticeably wider peaks. This is due to the angular and energy straggling that occurs when molecules break up into atomic fragments as they pass through the carbon foil that is the basis of the IMS TOF measurement [*Young et al.*, 2004]. The N^+ spectra peak [*Smith et al.*, 2005, 2007] is relatively narrow if it is produced only by atomic nitrogen ions. However, earlier, *Smith et al.* [2007] pointed out that in fact the N^+ peak is wider than predicted for a pure atomic N^+ source. If one assumes that contributions from molecular species widen the N^+ peak, then peak width analysis provides a method of detecting these molecular species.

[12] In order to increase TOF signal statistics from the LEF, we summed data from 26 orbits (Cassini orbits 3–29). We then binned these data according to distance from Saturn in Saturn radii or Rs (1 Rs ~ 60330 km). This data is an accumulation of 889 individual with the least amount of 43 spectra for the 4.5–5.0 Rs bin and a maximum of 175 spectra for the 5.5–6.0 radial bin. Additionally, we restricted the data to periods when Cassini was close to the equatorial plane (±0.25 Rs) to avoid compositional differences caused by scale height effects. Throughout this paper, we reference radial distance from Saturn, however because our data is in the inner magnetosphere and so close to the Saturn's equatorial plane, these result can also roughly be considered as dipole L-shell values as well. Data were further selected for periods when the instrument viewing angle is generally pointing at the corotational plasma flow. The latter is essential because the flux of ions is appreciable only from that direction. Since the "flow" at these low energies is due to ExB drift there is no mass selection effect.

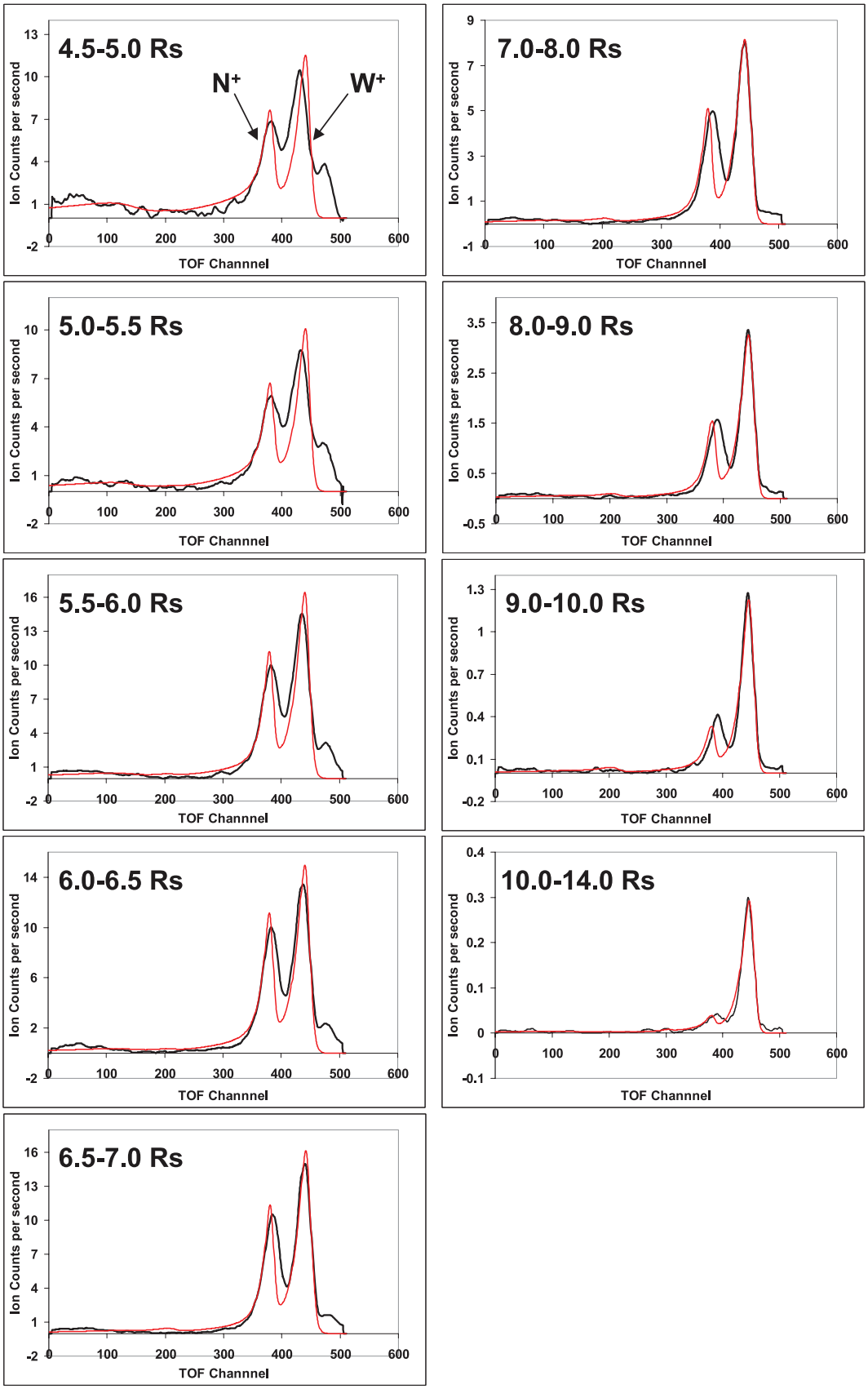

Figure 1. CAPS LEF spectra at 250 eV separated according to radial distance in Saturnian body radii (Rs). Black lines represent Cassini data, and red lines show the model fit to each spectrum. In the first panel, the spectral peaks associated with N^+ and W^+ (water group ions; O^+, OH^+, H_2O^+, and H_3O^+) are labeled. (The peak to the right of the W^+ peak currently eludes identification and may be an instrument effect.)

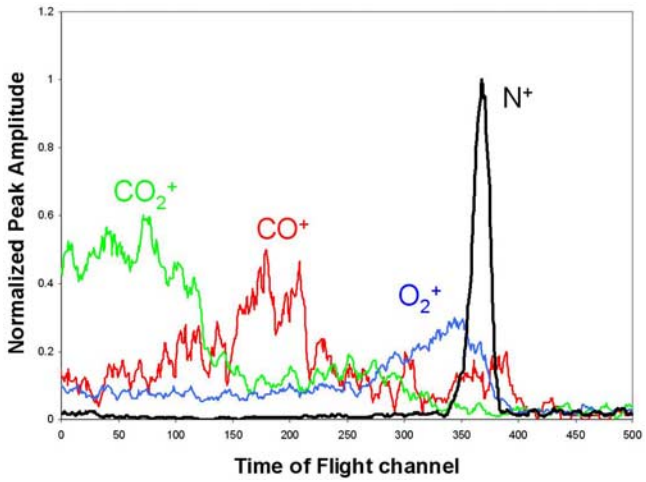

Figure 2. CAPS LEF calibration spectra taken at 250 eV. Spectra shown for N^+ (black line), O_2^+ (blue line), CO^+ (red line), and CO_2^+ (green line) as a function of normalized peak height and instrument time-of-flight channel.

[13] We divided the data into radial distance bins from Saturn because if Enceladus is producing ammonia, the relative abundance of molecular ions should decrease as a function of distance from the moon's orbit as the molecular ions are dissociated. One would, therefore, expect the nitrogen peak in the TOF spectra to become increasingly narrow as a function of radial distance from Enceladus' orbit.

[14] Figure 1 shows the spectra for the energy level that has the highest signal strength for all spatial bins (235 eV) separated by radial distance from Saturn between ~4.5 Rs and ~14 Rs. Appendix A provides more detail on the accuracy and methodology of these model fits. Below ~4.5 Rs, high-energy electrons cause increasing amounts of background signal. Beyond ~14 Rs the signal strength is too low for statistically meaningful identifications. The rightmost peak in each panel is created by oxygen daughter products from the breakup of water group ions ("W^+" includes O^+, OH^+, H_2O^+ and H_3O^+) while the left peak is the previously identified N^+ peak. In order to gain confidence in our analysis that N^+ peak widening is caused by ammonia products; we first must eliminate all other species that could contribute to the N^+ LEF peak. On the basis of results from calibration the species that could possibly widen the N^+ peak are O_2^+, CO^+, $^{15}N^+$ and NH_x^+ (x = 1–4). We assume $^{15}N^+$ is not present in detectable quantities because $^{15}N/^{14}N$ is <0.5% in solar, terrestrial and Titan concentrations [*Lammer et al.*, 2000; *Waite et al.*, 2005]. To illustrate LEF spectral peak shapes and their TOF locations we show CAPS calibration data taken at 250 eV for O_2^+, CO_2^+, CO^+ and N^+ (Figure 2). Notice that an O^+ fragment from an O_2^+ ion entering the instrument dissociating in the foil can widen the left shoulder of the N^+ peak, while CO^+ can similarly widen the right shoulder.

[15] To illustrate spectral peak widening caused by an increased fraction of molecular components, Figure 3 shows the full width at half maximum (FWHM, computed from the measured spectra) for the LEF water group ions shown in Figure 1 and other energies. The peak becomes narrower with increasing distance from Saturn, consistent with an increase in the amount of atomic ion components relative to molecular ions. This is because the primary source of heavy ions that compete with N^+ is H_2O from Enceladus. Over time and distance from the source, these molecules are scattered outward [*Johnson et al.*, 2006] and become dissociated, forming OH^+ and O^+ [e.g., *Jurac and Richardson*, 2005]. This causes the water group ion peak to become increasingly dominated by atomic species with increasing distance from the source thus resulting in a narrower TOF peak. We similarly examine the observed spatial trend in the N^+ peak width to determine if the same trend toward an atomic concentration is also present in the nitrogen peak.

[16] Before we consider the effect of NH_x^+ ions on the nominal N^+ peak, we applied a computational de-convolution algorithm to the spectra shown in Figure 1 and to similar data collected at 58, 83, 118, 167, 236 and 333 eV to account for other possible contributions in the spectra. Our program fits the spectra for CO_2^+, CO^+, O_2^+, N^+, N_2^+, C^+, H_2O^+, OH^+, O^+, and H_3O^+ by incrementally testing possible relative concentrations of each species and evaluating the quality of the total fit using the least squares method. The iteration with the lowest value is then deemed to have the best fit. While this de-convolution provides a good estimate of major species' abundances, it is more difficult to determine minor species (e.g., CO_2^+, CO^+, N_2^+ and C^+). Because O_2^+ abundances are known [*Martens et al.*, 2008], we have a high confidence in the amount of O_2^+ counts that must be removed (as indicated by our spectral deconvolution above and explained in Appendix A) from the N^+ peak to produce a "residual" N^+ peak. Figure 4 shows the full width half maximum (FWHM) of the residual N^+ peaks (same format as Figure 3) as a function of radial distance from Saturn for energies from 58 to 333 eV. Although at the smallest and largest radial distances there is large scatter, this plot shows a clear trend similar in the water-group ion FWHM presented above (Figure 3) where the peak becomes, on average, narrower as a function of radial distance from Saturn.

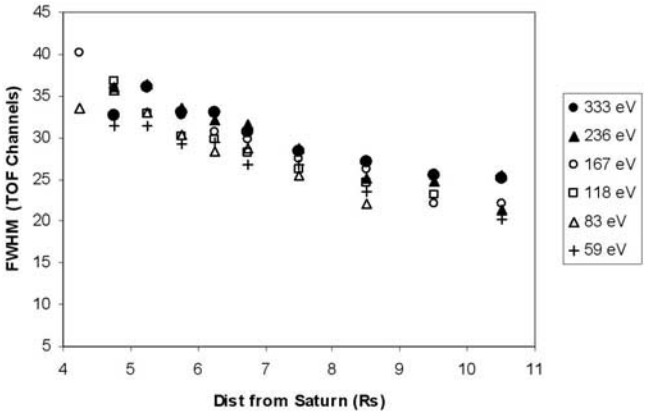

Figure 3. Spectral peak full width at half maximum (FWHM measured as the number of time-of-flight channel) for water group ions in CAPS LEF at various energies. Data are shown as a function of radial distance from Saturn (4.5 to >10 Rs).

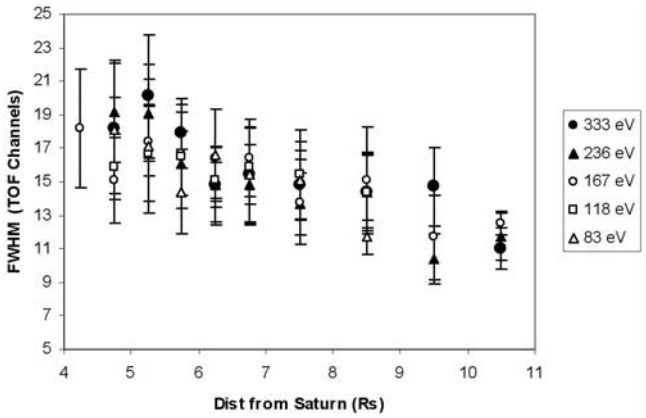

Figure 4. Spectral peak full width at half maximum (FWHM measured as the number of time-of-flight channel) for N^+ CAPS LEF. Data are shown as a function of radial distance from Saturn. These data represent the spectral peak width, with O_2^+ counts removed. Error bars represent 1-sigma errors.

[17] We now examine possible reasons for this observed behavior. A peak could widen because of a spread in ion energies contributing to the peak. We remove this effect by separating the data into specific energy bins so there is no energy dependence in the data. Peak narrowing occurs consistently in each energy band which provides confidence that widening does not occur as a result of changes in energy as a function of radial distance. Therefore, unless there is an unidentified instrument problem, peak widening should be caused by the presence of unidentified molecular ion species contributing to the N^+ peak. Additionally, the abundance of molecular species appears to decrease as a function of radial distance from Saturn, as indicated by the narrowing of the peak widths, which is consistent with observations of the water group peak. This indicates decreasing molecular contributions as Cassini moves further from Enceladus' orbit.

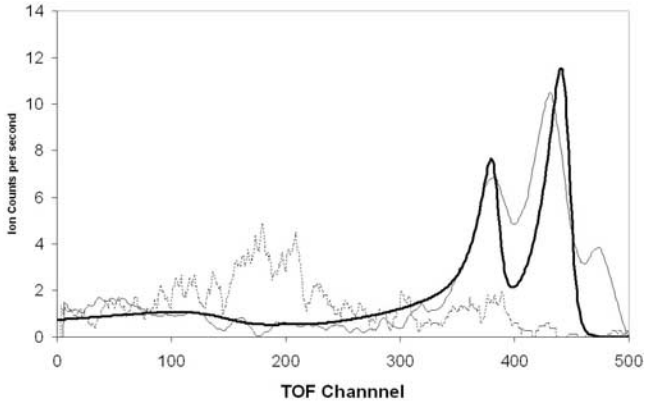

Figure 5. CAPS LEF data (thin line) collected from 4.5 to 5.0 planetary radii away from Saturn. The thick line shows the model fit to the spectrum for N^+, CO^+, CO_2^+, C^+, $O2^+$, O^+, OH^+, H_2O^+, and H_3O^+. TOF channels 1–250 are too low to justify the amount of CO^+ (dotted line) required to reproduce the observed N^+ spectra peak widening.

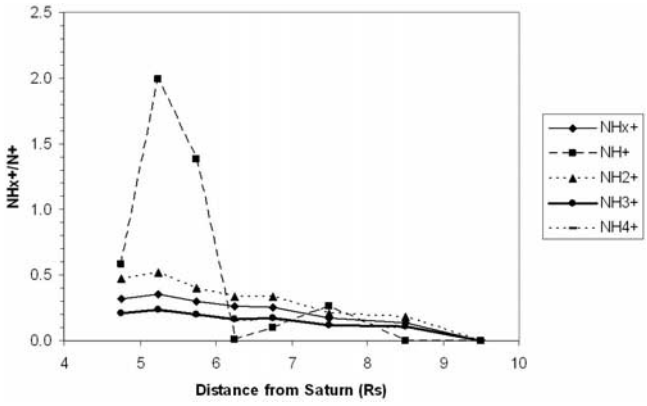

Figure 6. Upper limits on the ratios of ammonia-related species to the amount of N^+ (85–471 eV). The limits for NH^+ (dashed line with squares), NH_2^+ (dotted line with triangles), NH_3^+ (solid line with circles), NH_4^+ (dotted line with lines), and NH_x^+ combined (solid line with diamonds) are shown as a function of radial distance from Saturn (NH_4^+ is difficult to notice because it is approximately the same value as NH_3^+).

[18] To examine which molecules could contribute to the broadening, we simulate peak widening by adding molecular species other than NH_x^+ using model fits based on instrument calibration. Although we have already removed the best fit amounts of O_2^+ from the N^+ spectral peak, we now examine if it is possible to produce the observed peak widening by adding additional O_2^+ even though the fit would not be optimized. Therefore we examine whether there could be any additional contribution from O_2^+ (O^+ fragments from this species have approximately the same spectral TOF location as ammonia) that was not included in the initial correction discussed above. The amount of O_2^+ needed to produce the total change in peak width between the radial extremes (4.5 Rs and 14 Rs) requires an O_2^+/N^+ of ~2.4 at the maximum abundance location. Note that the approximate N^+ composition is $N^+/W^+ \sim 0.1$. For the change in N^+ peak width to be caused by additional O_2^+, the relative abundance of water-group ions would require an O_2^+/W^+ of ~0.24 (24%). However *Martens et al.* [2008] show that the total O_2^+ percentage always remains approx-

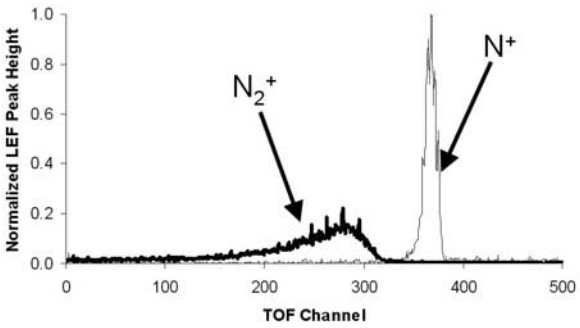

Figure 7. N^+ (thin line) vs. N_2^+ spectra (thick line) from calibrations at 64, 125, 250, and 375 eV. Data are averaged and then normalized to represent approximately equal amounts of both species.

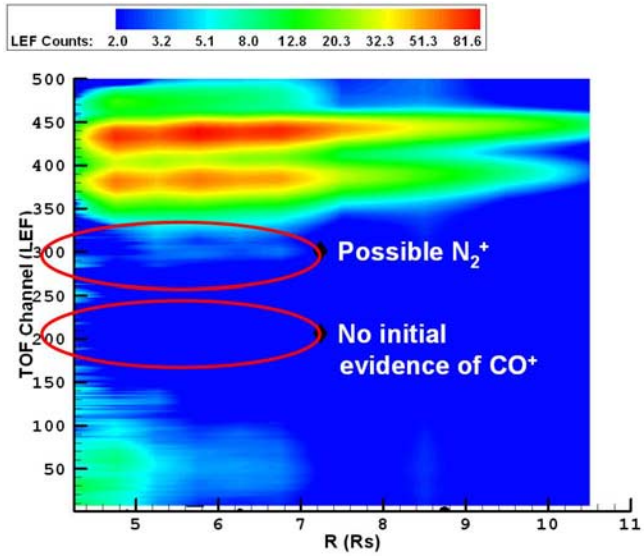

Figure 8. LEF spectrogram showing TOF vs. radial distance accumulated over 26 orbits. Ellipses indicate spectral regions where N_2^+- and CO^+-related products should appear.

imately less than 1%. Thus the presence of more O_2^+ cannot produce the observed N^+ peak widening in the inner magnetosphere without the presence of other molecular species.

[19] Next we consider CO^+. Our spectral de-convolution indicates the peak width widening would have to be caused by a CO^+/N^+ ratio of ~0.5. This equates to a CO^+ abundance of ~5% (of heavy ions) which is not an unreasonable amount of carbon monoxide based on the results of *Waite et al.* [2006]. However, assuming this amount of CO^+, calibration data (Figure 2) would predict a significant peak at the lower time-of-flight channels due to C^+ from CO^+, which is clearly not seen in the CAPS spectra (Figure 5).

[20] We have therefore eliminated O_2^+ and CO^+ as possible causes. Therefore we conclude that radially dependant N^+ peak widening should at least be partially caused by small amounts of ammonia-related species: i.e., NH_x^+ with x = 1–4. Because the CAPS sensitivity for each of these species is similar, we have forward fit the spectra for NH^+, NH_2^+, NH_3^+, NH_4^+ and equal amounts of each species to set an upper limit on the amount of ammonia products present. Figure 6 summarizes these upper limits as a function of radial distance from Saturn. Therefore the data in Figure 6 show the increasing amount of ammonia products required to fit the data as Cassini moves closer to Enceladus' orbit.

[21] To better characterize the contribution of the various ammonia fragment ions to the nitrogen peak, we first examine NH^+. We find it is difficult to produce the observed peak widening with only NH^+. However, if we assume, unrealistically, that the peak width broadening at the point closest to Enceladus' orbit is only caused by NH^+, it can almost be reproduced with >200% of NH^+ relative to N^+ (or >20% of the total heavy ion concentration). Given the high density of NH^+ required, we should be able to detect NH^+ using the ST detector but no detection is evident. Therefore we are confident that NH^+ alone is not responsible for the observations. NH_2^+ can cause the observed peak widening at the closest point with a 0.5 ratio of NH_2^+ to N^+ (equivalent to an upper limit of ~5% of the total heavy ion concentration—which again seems high because this much NH_2^+ should be more obvious in the other detector). On the other hand, NH_3^+ requires a ratio of only ~0.2 upper limit (or ~2% of the total density with a 10% concentration of N^+) for data closest to Enceladus. The NH_4^+ upper limit is also ~0.2 in this region. As a first examination of a multi-species composition, we attempt to fit the spectra with all of these species in equal proportions and derive an upper limit for ammonia products near Enceladus of NH_x^+/N^+ ~0.35 (~3.5% of the heavy ions). This is equivalent to ~0.09 for each species individually (~1% of total heavy ions).

3. Molecular Nitrogen

[22] *Smith et al.* [2005] detected N^+ in Saturn's inner magnetosphere but did not detect N_2^+. However, considering the INMS mass 28 detection in the Enceladus plume [*Waite et al.*, 2006], *Smith et al.* [2007] developed a neutral cloud model assuming N_2 in the plume is the source of detected N^+. Ignoring the peak width discussion above, they showed that the observed N^+ could be produced by an N_2 plume source, but they could not confirm that N_2 was required to produce the observed N^+. Therefore we now examine more closely the CAPS ability to detect low concentrations of N_2^+.

[23] After normalizing N_2^+ and N^+ calibration data for incoming flux rate, an interesting picture emerges. Figure 7 shows the normalized TOF calibration spectra for N^+ fragments from N^+ and N_2^+ at 64, 125, 250 and 375 eV. While both peaks represent the same number of ion detections, molecular fragments have a wider TOF dispersion than

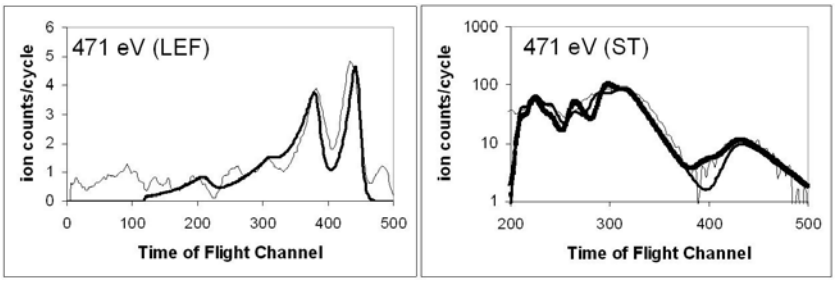

Figure 9. TOF data per collection cycle for CAPS (left) LEF and (right) ST. Data were accumulated at 4.0–5.5 Rs at 471 eV. Thin black lines are CAPS data; thick lines are the model fits with N_2^+. The ST medium thickness line is the model fit without N_2^+.

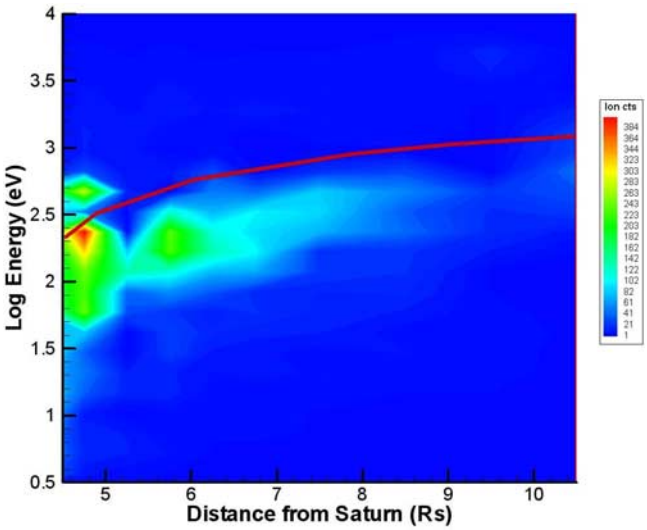

Figure 10. CAPS ST potential mass 28 detections (in ion counts) as a function of energy and radial distance from Saturn (in Saturn radii). The red line shows the mass 28 corotational energy.

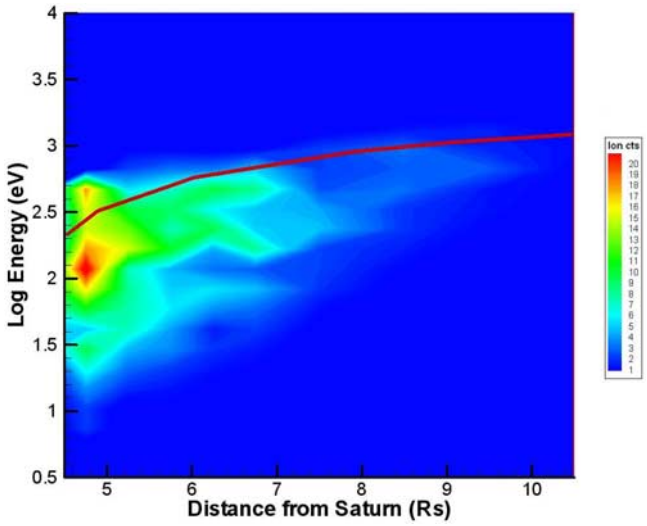

Figure 11. CAPS LEF potential N_2^+ detections (in ion counts) as a function of energy and radial distance from Saturn (in Saturn radii). The red line shows the N_2^+ corotational energy.

atomic fragments. This dramatically spreads the travel time to the detector for the N^+ daughter fragment produced by N_2^+ incident on the carbon foil. As shown in Figure 7 the result is that the amplitude of N_2^+ is only 22% of the N^+ peak. Therefore, for the same amounts of N_2^+ and N^+, the peak associated with N^+ from molecular nitrogen has much lower amplitude and is much broader, making the signal/noise ratio smaller and therefore the peak more difficult to detect. This is especially a problem close to Enceladus orbit where both molecular ion component and the background would be expected to be largest. These results indicate that N_2^+ in the CAPS data of comparable amounts to N^+ at current signal strengths would be difficult to identify.

[24] To further investigate the presence of N_2^+, we return to the spatially ordered LEF spectra in Figure 1 where we were able to identify potentially small amounts of N_2^+. Figure 8 shows a spectrogram of the data presented in Figure 1 to illustrate that these data indicate the possible presence of N_2^+ closer to Saturn but no obvious indication of CO^+. This allows for the possibility of N_2^+, but does not confirm its presence. The situation is further complicated because C^+ would also appear at approximately the same location. To gain more insight into the composition we also examine data from the Straight-through (ST) detector which has lower mass resolution as the LEF but has higher detection efficiency. Although the ST is not well suited for separating CO^+ from N_2^+, it can help determine the presence of an aggregate of mass 28 species. Unfortunately detection of mass 28 is hindered because its location is very close to mass 32 (O_2^+) which has been detected [*Young et al.*, 2005; *Tokar et al.*, 2005; *Johnson et al.*, 2006; *Martens et al.*, 2008].

[25] Figure 9 shows example LEF (left) and ST (right) spectra for data integrated from 4.0–5.5 Rs. This figure shows the ST data fit is better using mass 28 (Chi-squared improvement of ~1%) while the LEF data allows for a possible but not confirmed N_2^+ presence. We also deconvolved the ST and LEF data using the method described above and identified all of the possible locations in the data where mass 28 (ST) and N_2^+ (LEF) could contribute to the peaks seen in the ST and the LEF data at the same concentrations. Figure 10 shows the locations by energy where mass 28 can be fit into the ST data with an improved chi-squared fit of ~1% The red lines show the spatially dependent N_2^+ corotational energy or the approximate energy that newly generated N_2^+ should obtain if ionization occurred at that location. Additionally, Figure 11 shows the locations by energy where N_2^+ can be fit into the LEF data. These figures show that the potential N_2^+ detections occur in both CAPS IMS detectors at energies lower than pick-up energies.

[26] We also examined the ST data collected during Enceladus encounters and orbit crossing (day 195 & 67 2005) more closely and although the data supports the presence of small amounts of mass 28, the large amount of noise in this region makes a conclusive determination

Table 1. Upper Limits as a Function of Radial Distance From Saturn in Planetary Radii (Rs)[a]

Rs	ST Mass 28 Upper Limit (% of Heavy Ions)	LEF N^{2+} Upper Limits (% of Heavy Ions)	LEF Best Fit N_2^+/CO^+
4.0–4.5	*	3.6	1.23
4.5–5.0	2.8	2.7	0.28
5.0–5.5	1.6	2.5	0.20
5.5–6.0	2.0	1.9	0.15
6.0–6.5	1.3	1.7	0.20
6.5–7.0	1.9	1.9	0.23
7.0–8.0	2.2	1.5	0.21
8.0–9.0	2.5	1.6	0.23
9.0–10.0	1.8	1.2	0.16
>10.0	2.7	1.2	*

[a]First column is for mass 28 based on CAPS ST data, and second column is for N_2^+ based on CAPS LEF data (as a percentage of the total heavy ion population). Third column is the CAPS LEF best fit for N_2^+ and CO^+ (ratio of the amount of N_2^+ to CO^+). Asterisk indicates data not available.

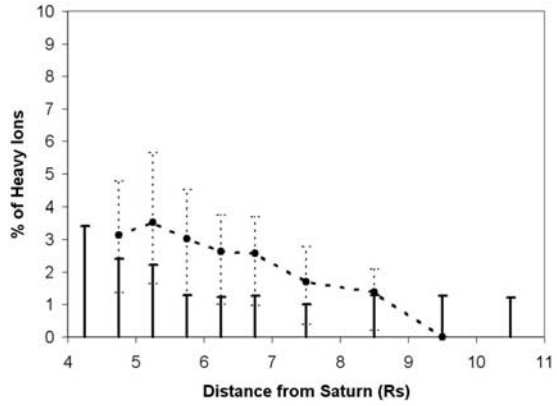

Figure 12. Upper limit for N_2^+ and NH_x^+ based on CAPS LEF observations. Results shown as the upper limit N_2^+ (solid black lines) and NH_x^+ (dotted line) percentage of all heavy ions as a function of radial distance from Saturn in planetary radii (Rs). Error bars represent 1-sigma errors for peak widths. (Enceladus orbits at ~4 Rs, while Titan is ~20 Rs from Saturn.)

difficult. Our detections therefore represent an upper limit on the amount of N_2^+ possible in the data. We summarize the spatially dependent upper limits for Mass 28 based on CAPS ST data (as a percentage of the heavy ions) shown in Table 1. Note that the N_2^+ spectral peak location is very different from the N^+ peak discussed above. Likewise, Table 1 also shows the upper limit for N_2^+ in the CAPS LEF detector based on the spectral de-convolution process mentioned above. Additionally, based on the CAPS LEF detector we computed a best fit N_2^+/CO^+ ratio to the spectra as shown in Table 1. Also note that while Figure 8 shows that CAPS spectra do not contain enough CO^+ to explain the N^+ peak widening, the spectra do potentially allow for small amounts of CO^+ as indicated in Table 1. Finally, we then constrain the upper limits on N_2^+ as shown in Figure 12. Note, as mentioned above, penetrating background radiation causes larger uncertainty in our results for data obtained closer to Saturn.

4. Discussion

[27] Our goal was to determine the possible molecular parents of N^+ detected in Saturn's inner magnetospheric plasma. The analysis of the N^+ spatial and energy distribution presented here suggests a source close to Enceladus' orbit and is consistent with our earlier results [*Smith et al.*, 2005, 2007]. The INMS detected mass 28 in the Enceladus plume [*Waite et al.*, 2005], which they initially suggested was N_2 but could also be CO. Therefore we first considered the existence of molecular nitrogen. We cannot directly confirm N_2^+ is present using the CAPS ion data but arguments presented here show that it could still be present and be indiscernible from the CAPS background because of a combination of low-incident fluxes of N_2^+ and detector efficiencies especially near Enceladus. Therefore we have used both ion mass detectors on the CAPS to place upper limits on the amount of this species. Although, as stated, these are not confirmed detections we show the observed spectra are fitted better by including small amounts of N_2^+ (<3.6% of total heavy ion population) and also possibly CO^+.

[28] Figure 9 shows that TOF spectra are best fit with mass 28 in the ST detector and, although the data are noisy, the LEF spectra can allow for a small amount of N_2^+. Using these results, we show the possible energy distribution of N_2^+ vs. distance from Saturn in Figures 10 and 11. The trend is similar to the pick-up ion energy, only shifted to lower energies.

[29] On the basis of this research we are able to place upper limits on the amount of mass 28 possible as a percentage of the heavy ion population (Figure 12). While this only represents an upper limit, the results are consistent with a potential Enceladus source. However we do experience more interference from background radiation at closer distances to Saturn. We tried to further constrain this detection by showing the spectral best fit ratio of N_2^+ to CO^+. The fit consistently shows that the spectra are best fit with at least some N_2^+ (<3.6%) in the spectra. The ratio also seems to favor a higher amount of N_2^+ closer to Enceladus' orbit, however this is also the region where CAPS experiences the most interference from penetrating radiation (discussed above) so these upper limits do not necessarily confirm a higher amount of N_2^+ closer to Enceladus. By combining all of these results, we were able to produce N_2^+ upper limits as a function of distance from Saturn (Figures 10 and 11) showing that the upper limits increase closer to Enceladus which is consistent with the N_2 source model constructed by *Smith et al.* [2007]. As a cross instrument confirmation of these results, the N_2^+ upper limit closest to Enceladus is ~4% which is similar to the value of mass 28 percentage reported by *Waite et al.* [2005] in the Enceladus plume.

[30] We also showed the results of our NH_x^+ research. As mentioned earlier, the location and potential relative abundance of NH_x^+ prevents us from making a direct detection or de-convolution of these species in the CAPS spectra. However, our examination of the N^+ peak width produces results that indicate the presence of these species. The results in Figure 4 show the N^+ peak is noticeably wider as we move closer to Enceladus' orbit. This is interesting because the atomic species generate noticeably narrower spectral peaks than molecular species in the CAPS LEF detector.

[31] We examined these data independently for each specific energy pass band to remove the possibility that differences in energy distribution could cause the peak to become wider with distance from Saturn. Because we observe the same peak width changes independently at each energy level, energy distribution changes cannot explain the trend. We also determined that no currently identified issue with the detector could produce such an effect. Therefore, assuming there is not some unknown detector issue, this change in N^+ spectra peak width should be caused by changes in the molecular vs. atomic species concentration.

[32] The possible molecular species that could contribute to this N^+ peak are O_2^+, CO^+ and NH_x^+ (x = 1–4). O_2^+ has already been detected and shows a fairly conclusive fit in the spectra. Therefore we fit the spectra for O_2^+ and removed these counts from the N^+ spectra peak to produce a "residual" N^+ spectral peak. Even with the O_2^+ removed, the N^+ peak still shows a spatially dependent peak width.

We then determined that there are insignificant amounts of CO^+ or O_2^+ fragments contributing to the peak width. We therefore propose that the narrowing peak width with increasing distance from Enceladus is due to the increase in the dissociation of ammonia with distance from Enceladus. Testing this assumption, we simulate the peak widening using NH^+, NH_2^+, NH_3^+ or NH_4^+ to place limits on the amount of these species that can be present. Assuming the N^+ spectra peak is composed almost entirely of atomic nitrogen (as suggested by the CAPS spectra models) beyond ~10 Rs, Figure 6 shows the relative amount of ammonia product ions that are present in the plasma close to Enceladus' orbit. Additionally, assuming the residual peak width is only caused by equal amounts of ammonia-group ions, we show this abundance (as a percentage of the heavy ion population) relative to the N_2^+ upper limits (as a function of distance from Saturn) in Figure 12.

[33] There is also a possibility that NH^+ could be produced in the plasma by an ion molecule reaction of N^+ or N_2^+ with water products. However it is very difficult to reproduce the observed spectral peak widening with only NH^+. Therefore it appears likely that other NH_x^+ must be present.

5. Summary and Future Work

[34] In this paper, we expand on the work of *Smith et al.* [2007] to identify the source molecules for nitrogen ions detected in Saturn's inner magnetosphere. We conducted an extensive study of all available CAPS data to determine if N_2^+ or ammonia were the parent molecules for these nitrogen ions detected by Smith et al. in Saturn's magnetosphere. We present evidence for the detection of product ions (NH_x^+) likely from ammonia We find that in order to explain our observations, if only one of these species is present, as a percentage of heavy ions, there needs to be ~3.4% of NH_2^+, ~2.0% of either NH_3^+ or NH_4^+. Alternatively, if all four species are added in equal proportions, there only needs to be ~0.7% of each to explain the spectral behavior we observed.

[35] Because the INMS detected neutral particles with an atomic mass of 28 but could not determine how much of this is from ionization of N_2 or CO, we also looked for evidence for N_2^+. Although we could not positively confirm the presence of N_2^+ in Saturn magnetosphere through direct observation, we showed that a best fit to the CAPS data is obtained when including small amounts of N_2^+. Also, we placed upper limits on the amount of mass 28 as well as the amount of N_2^+. Interestingly, the upper limit we place on the amount of N_2^+ close to Enceladus' orbit is similar to the INMS mass 28 detection (~4%). Also of interest, the radial distribution of our N_2^+ upper limits follows the trends modeled by Smith et al. for N_2 in the Enceladus plumes.

[36] The indications of ammonia products and upper limits on N_2^+ suggest that both ammonia and molecular nitrogen are emitted from Enceladus. This result now can be used to constrain the subsurface processes and composition of Enceladus. Further analysis of these data is underway and once Cassini returns to equatorial orbit in 2009, additional observations will be available. Considering the upcoming close encounters with Enceladus and well as occultations, Cassini observation should be able to build on the understanding of molecular sources of nitrogen considered here.

Appendix A: Time of Flight Spectra and Model Fitting Details

A1. CAPS Spectra TOF Channels

[37] The CAPS TOF spectra is measured in 2048 time-of-flight channels [*Young et al.*, 2004] however only 512 channels of these data are sent back to Earth because of data band width constraints. The channels sent back to Earth are selected to focus on the mass region of the spectra most important to the specific Saturnian region being studied. The *Young et al.* [2004] instrument paper however divides the TOF channel numbers by four. For this paper, we plot data by radial distance form Saturn. The CAPS LEF spectra in this article coincides with TOF channels 650 to 1161 (i.e., original TOF channel 650 is channel 0 in this paper) and the CAPS ST spectra start with TOF channel 40 and then selects every second channel afterward. We have adjusted the calibration TOF channels to coincide with the operational data channels.

A2. Spectral Model Fitting Methodology

[38] Model fits to the CAPS spectra are created by comparing data obtained from NASA Goddard Space Flight Center, Los Alamos National Lab and Southwest Research Institute calibration experiments using a prototype version of the CAPS as well as the fight model onboard Cassini. These tests were conducted prior to launch for over 20 atomic and molecular ion species at multiple energy levels resulting in hundreds of calibration spectra.

[39] In order to translate these data into a form that can be used to deconvolve species in the operational spectra, we use a Logistic Power Peak Model, LPP, represented by:

$$LPP(\chi) = \frac{a^*}{d}\left[1 + e^{\left(\frac{\chi + c^* \ln(d) - b}{c}\right)}\right]^{\frac{-d-1}{d}} * \left[e^{\left(\frac{\chi + c^* \ln(d) - b}{c}\right)}\right] * (d+1)^{\frac{d+1}{d}} \tag{A1}$$

Each ion species is defined by four parameters where "a" is the fragment probability, "b" is the peak center location, "c" is the peak width and "d" relates to peak asymmetry. These parameters are defined with parametric relationships based on calibration data using total molecule mass, fragment mass and particle energy. Using these equations, we produce spectra model fits for H_3O^+, H_2O^+, OH^+, O^+, N_2^+, C^+, CO^+, CO_2^+, O_2^+, N^+, NH^+, NH_2^+, $NH_3^+$and NH_4^+. We then use a computational program that iteratively adjusts the relative amounts of each of these species and combines these model spectra into single simulated spectrum that is compared to the operational CAPS data. The quality of each model fit is determined using a "reduced chi-squared" (χ^2) method. This method assesses the quality of a model fit using the equation:

$$\chi^2 = \frac{\sum_{i=1}^{n}\left(\frac{CAPS_i - LPP_i}{LPP_i}\right)}{(n-1)} \tag{A2}$$

where there are n TOF channels and $CAPS_i$ and LPP_i represent the number of counts at channel i in the

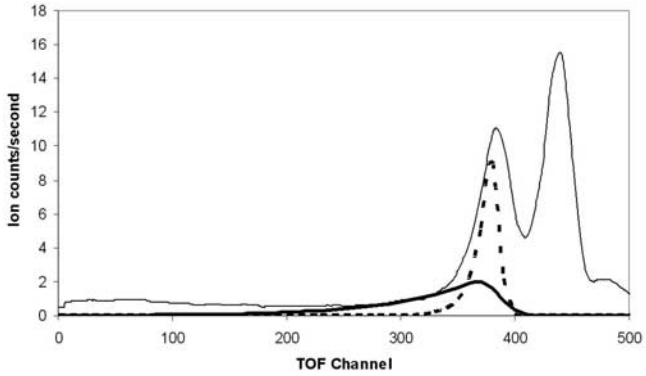

Figure A1. CAPS LEF data (thin line) collected from 6.5 to 7.0 planetary radii away from Saturn. The dotted line shows the model fit to the spectrum for N^+, and the thick line shows the fit for O_2^+. For this example, the O_2^+ peak amplitude is approximately 18% for the N^+ amplitude.

operational and calibration spectra, respectively. The iteration with the lowest value of χ^2 indicates the best fit to the spectra. The resulting abundances for each species constitute our spectral de-convolution. The χ^2 results for Figure 1 are: 0.43 (4.5–5.0 Rs), 0.29 (5.0–5.5 Rs), 0.37 (5.5–6.0 Rs), 0.35 (6.0–6.5 Rs), 0.38 (6.5–7.0 Rs), 0.24 (7.0–8.0 Rs), 0.09 (8.0–9.0 Rs), 0.02 (9.0–10.0 Rs) and 0.01 (10.0–14.0 Rs).

[40] While the chi-squared method provides the quality of a model fit, we also account for the statistical error in the operational data by computing the uncertainty of each peak using the "fractional 1σ" method, defined by:

$$(1\sigma) = \sqrt{\left(\sum_{i=1}^{n}\right)\left[\frac{\sqrt{CAPS_i}}{CAPS_i}\right]^2} \qquad \text{(A3)}$$

[41] This gives the probability that the actual numbers are within ±1 sigma (34.1%) of the observed count numbers. We use these values to set upper limits (and lower limits of zero) for the molecular nitrogen fitting results.

A3. FWHM Methodology

[42] For the FWHM analysis, we determine the ion counts in each time-of-flight channel for O_2^+ (as determined by the model fitting above). Because this species contributes to the same spectra peak as N^+ and ammonia products, we remove these ion counts from the CAPS spectra (>10% of the total counts for all spectra). The remaining peak is a modified LEF N^+ spectral peak with the expected O_2^+ ion counts removed. Figure A1 shows a sample spectra with the N^+ and O_2^+ contributions identified.

[43] We next focus on analysis of this modified CAPS data only. Using an off the shelf peak fitting computational program, we fit a curve to the data (independent of the model constraints above) and calculate the full width and half maximum of each nitrogen spectral peak.

[44] We calculate the FWHM uncertainty by generating a synthetic LEF spectrum with 1-sigma counts added to the spectrum. We then compute the FWHM of these increased spectra which represent the upper limit error bars for our FWHM results. Similarly, we remove the 1-sigma error counts from the spectra to determine the lower limit 1-sigma FWHM error.

A4. Modeling Fitting Issues

[45] The CAPS model fits (above) must rely heavily on prototype instrument calibration data rather than flight instrument spectra because more data exists for the former instrument. It is known that spectra from these two instruments vary in terms of TOF channel locations for each species. Because water group ions are much more abundant than other heavy species, the "peak shift" between the two instruments is well understood and thus the water group peak fits are better in Figure 1 than the N^+ peak. However, the instrument team is becoming more confident in these model fits and we have examined in detail the offset in the N^+ peak and cannot find any ion species that can cause the excess counts on the right side of the nitrogen peak. Therefore it is likely model fits for this peak need to be slightly adjusted. However, this shift is not yet conclusively agreed on so we show the model fits in Figure 1 using the current models although we have confidence these counts are attributed to N^+.

[46] In order to increase confidence in our results, we defined our FWHM technique of the N^+ peak so that this likely peak shift is not a factor in our analysis which is independent of the exact peak location. Additionally, the asymmetric tail of spectra begins at a height far below the 50% height and should not affect the analysis. Our N_2^+/mass 28 analysis uses spectra peaks that are located in TOF channels which allows use of both CAPS IMS detectors (LEF & ST). This cross analysis increases confidence in our model fits. Therefore out results should not be affected by further minor refinements of the CAPS spectra models.

[47] **Acknowledgments.** This work is supported by JPL contract 1243218 with SwRI for CAPS operations and data analysis, MIMI operations and data analysis, the NASA Planetary Atmospheres and Outer Planets Programs, NASA GSRP, and the Virginia Space Grant Consortium. This work is also partially supported by NASA Contract NAS5-97271 Task Order 003.

[48] Wolfgang Baumjohann thanks the reviewers for their assistance in evaluating this paper.

References

Barbosa, D. D. (1987), Titan's atomic nitrogen torus: Inferred properties and consequences for the Saturnian aurora, *Icarus*, *72*, 53–61.

Ip, W. (1997), On neutral cloud distributions in the Saturnian magnetosphere, *Icarus*, *97*, 42–47.

Johnson, R. E., H. T. Smith, O. J. Tucker, M. Liu, M. H. Burger, E. C. Sittler Jr., and R. L. Tucker (2006), The Enceladus and OH tori at Saturn, *Astrophys. J. Lett.*, *644*, L137–L139.

Jurac, S., and J. D. Richardson (2005), A self-consistent model of plasma and neutrals at Saturn: Neutral cloud morphology, *J. Geophys. Res.*, *110*, A09220, doi:10.1029/2004JA010635.

Lammer, H. A., W. B. Stumptnera, G. J. D. Molina-Cuberosc, S. J. Bauera, and B. T. Owen (2000), Nitrogen isotope fractionation and its consequence for Titan's atmospheric evolution, *Planet. Space Sci.*, *48*(6), 529–543.

Lanzerotti, L. J., W. L. Brown, K. J. Marcantonio, and R. E. Johnson (1984), Production of ammonia-depleted surface layers on the Saturnian satellites by ion sputtering, *Nature*, *312*, 139–140.

Martens, H. R., D. B. Reisenfeld, J. D. Williams, R. E. Johnson, and H. T. Smith (2008), Observations of molecular oxygen ions in Saturn's inner magnetosphere, *Geophys. Res. Lett.*, *35*, L20103, doi:10.1029/2008GL035433.

Matson, D. L., J. C. Castillo, J. Lunine, and T. V. Johnson (2007), Enceladus' plume: Compositional evidence for a hot interior, *Icarus*, *187*(2), 569–573.

Nimmo, F., and R. T. Pappalardo (2006), Diapir-induced reorientation of Saturn's moon Enceladus, *Nature*, *441*(7093), 614–616.

Porco, C. C., et al. (2006), Cassini observes the active south pole of Enceladus, *Science*, *311*(5766), 1393–1401.

Smith, H. T., R. E. Johnson, and V. I. Shematovich (2004), Titan's atomic and molecular nitrogen tori, *Geophys. Res. Lett.*, *31*, L16804, doi:10.1029/2004GL020580.

Smith, H. T., M. Shappirio, E. C. Sittler, D. Reisenfeld, R. E. Johnson, R. A. Baragiola, F. J. Crary, D. J. McComas, and D. T. Young (2005), Discovery of nitrogen in Saturn's inner magnetosphere, *Geophys. Res. Lett.*, *32*, L14S03, doi:10.1029/2005GL022654.

Smith, H. T., R. E. Johnson, E. C. Sittler, M. Shappirio, D. Reisenfeld, O. J. Tucker, M. H. Burger, F. J. Crary, D. J. McComas, and D. T. Young (2007), Enceladus: The likely dominant nitrogen source in Saturn's magnetosphere, *Icarus*, *188*(2), 356–366.

Squyres, S., R. Reynolds, and P. Cassen (1983), The evolution of Enceladus, *Icarus*, *53*, 319–331.

Stevenson, D. J. (1982), Volcanism and igneous processes in small icy satellites, *Nature*, *298*, 142–144.

Tokar, R. L., et al. (2005), Cassini observations of the thermal plasma in the vicinity of Saturn's main rings and the F and G rings, *Geophys. Res. Lett.*, *32*, L14S04, doi:10.1029/2005GL022690.

Verbiscer, A. J., D. E. Peterson, M. F. Skrutskie, M. Cushing, P. Helfenstein, M. J. Nelson, J. D. Smith, and J. C. Wilson (2006), Near-infrared spectra of the leading and trailing hemispheres of Enceladus, *Icarus*, *188*(1), 211–223.

Waite, J. H., et al. (2004), The Cassini Ion and Neutral Mass Spectrometer (INMS) investigation, *Space Sci. Rev.*, *114*, 113–231.

Waite, J. H., et al. (2005), Ion neutral mass spectrometer results from the first flyby of Titan, *Science*, *308*(5724), 982–986.

Waite, J. H., et al. (2006), Cassini Ion and Neutral Mass Spectrometer: Enceladus plume composition and structure, *Science*, *311*(5766), 1419–1422.

Young, D. T., et al. (2004), Cassini plasma spectrometer investigation, *Space Sci. Rev.*, *114*, 1–112.

Young, D. T., et al. (2005), Composition and dynamics of plasma in Saturn's magnetosphere, *Science*, *307*, 1262–1264.

F. J. Crary, D. J. McComas, and D. T. Young, Division of Space Science and Engineering, Southwest Research Institute, 9503 W Commerce, San Antonio, TX 78227-1301, USA.

R. E. Johnson, Engineering Physics, University of Virginia, Thornton Hall, Charlottesville, VA 22904, USA.

D. Reisenfeld, Department of Physics and Astronomy, University of Montana, 32 Campus Drive, Missoula, MT 59812, USA.

M. Shappirio and E. C. Sittler, NASA Goddard Space Flight Center, 8800 Greenbelt Road, Greenbelt, MD 20771, USA.

H. T. Smith, Applied Physics Laboratory, Johns Hopkins University, 11100 Johns Hopkins Road, MP3-E175, Laurel, MD 20723, USA. (h.todd.smith@jhuapl.edu)